DOI 10.1007/s11085-017-9775-8

NaCl-Induced High-Temperature Corrosion of β21S Ti Alloy

Clément Ciszak[1] · Ioana Popa[1] · Jean-Michel Brossard[2] · Daniel Monceau[3] · Sébastien Chevalier[1]

Abstract Titanium alloys are very interesting for aeronautics applications because of their low density, high mechanical resistance and good resistance to corrosion in aggressive environments. However, recent developments impose the use of these materials at higher temperatures than those initially envisaged (above 400 °C), revealing some uncertainties of their behavior. Depending on the operating conditions, the material can be exposed to variable humidity levels and, in some cases, can be in contact with silica or marine salt. This study aims to evaluate the influence of NaCl solid deposit on the behavior of β21S Ti alloy at 560 °C under realistic ambient atmospheres. The tests were carried out in laboratory air and in water vapor-enriched air, on uncoated samples and on samples with solid NaCl deposit. The reaction-product evolution (up to 600 h) was characterized by thermogravimetric analysis, SEM observations (surface and cross section), XRD and microhardness profiling on cross sections. An aggravation of the corrosion phenomena in

✉ Ioana Popa
ioana.popa@u-bourgogne.fr

Clément Ciszak
clement.ciszak@u-bourgogne.fr

Jean-Michel Brossard
jean-michel.brossard@veolia.fr

Daniel Monceau
daniel.monceau@ensiacet.fr

Sébastien Chevalier
sebastien.chevalier@u-bourgogne.fr

[1] ICB, UMR 6303 CNRS – Université de Bourgogne Franche-Comté, 9 Avenue Savary, 21078 Dijon, France

[2] Veolia Recherche et Innovation, 291 Avenue Dreyfous-Ducas, 78520 Limay, France

[3] CIRIMAT, Université de Toulouse, CNRS, INPT, UPS, ENSIACET 4 allée Emile Monso, BP-44362, 31030 Toulouse Cedex 4, France

the presence of NaCl solid deposit was observed, that was related to the presence of gaseous metal chlorides, leading to the establishment of an active corrosion process.

Keywords Ti alloy · NaCl solid deposit · High-temperature corrosion · Oxygen dissolution

Introduction

Ti-based alloys have been increasingly used in various domains such as chemical industry, medical engineering and aerospace for their high corrosion resistance, biocompatibility, high specific strength and low density. However, they are sometimes asked to work beyond their original limits, especially in terms of thermal stresses, revealing uncertainties about their behavior at high temperature. Moreover, depending on the operating conditions, the material behavior can significantly be influenced by the presence of humidity in the gaseous environment or by the contact with marine salt at the surface.

The main oxidation product of titanium alloys when exposed to air at high temperature is TiO_2 rutile that grows by inward diffusion of the oxygen ions [1]. In parallel, the high solubility of oxygen in titanium (up to 33%) leads to the formation of an underlying oxygen-rich layer inside the base metal, often called α-case in α or $\alpha + \beta$ alloys [1, 2]. This O-enriched layer is less ductile and might affect the mechanical properties of the Ti substrate. The oxidation behavior of Ti alloys was found to be improved when alloying elements such as Al, Zr, Si, Cr, Nb, Ta, W and Mo are present in their composition [1, 3].

The presence of water vapor in the atmosphere leads to an increase of the mass gain with increasing water vapor pressure and with increasing temperature between 650 and 900 °C [4, 5]. At temperatures of 600 °C, a positive effect of the water vapor on the oxidation behavior was observed by Champin et al. [3]. In dry air, the oxidation kinetics is governed by parabolic laws at intermediate temperatures (600–700 °C), while at higher temperatures breakaway to linear kinetics is observed after extended exposure [6]. In moist air, the initial linear oxidation kinetics changes to parabolic after a time depending on the exposure temperature [5]. Different kinetics are associated with different morphologies of the oxide scales and different growth mechanisms. Moist air corrosion scales contain pores and/or whiskers at the outer part [7], which are typical of water vapor presence [8].

According to Stringer et al. [9], the oxidation behavior is controlled by rutile oxide growth at temperatures below 600–650 °C, while the dissolution of oxygen in the alloy controls the oxidation rate at higher temperatures. Perez et al. [10] showed that, at temperatures higher than 700 °C, the oxygen dissolution area in pure titanium increases in moist air compared to dry air.

The effect of solid NaCl deposit at the surface of Ti alloys during their exposure at high temperature in dry air or moist air is much less studied in the literature. However, several authors showed an enhancement of the oxidation rate in dry air in the presence of NaCl [11–13]. This increase is even more important when humidity is added in the exposition environment [12, 14, 15]. In both cases, the resulting

corrosion layers are much thicker, porous, affected by cracks and non-adherent to the metallic substrate. The oxidation scales are generally formed of TiO_2 rutile and Na–Ti mixed oxides and may contain oxides of the alloying elements. In some cases, Cl could be observed in the internal part of the oxide scale, ahead of the oxidation front. This observation suggests the formation of a transient titanium chloride that is subsequently oxidized to the more stable TiO_2 [12]. In parallel, the depth of the oxygen dissolution area equally increases with the exposure temperature and the severity of the exposure environment. Oxygen can penetrate into alloy at a faster rate because of volatile chlorides formation that induces cracking of the oxide scale [2].

Some authors propose oxidation mechanisms of Ti alloys in the presence of NaCl solid deposits [14–17]. These mechanisms are based on thermodynamical calculations, but not proven experimentally. They are based on reactions involving O_2 from atmosphere and the deposited NaCl, leading to the release of Cl_2 in parallel with the formation of TiO_2 and $NaTiO_2$ (or Na_2TiO_3) mixed oxides. The reactions are established with solid NaCl [15, 16] or with gaseous NaCl [14, 17]. In the presence of moisture, the oxidation mechanisms involve the formation of TiO_2 and Na_2TiO_3 oxides with release of HCl and H_2 gaseous species [14, 16]. The synergistic harmful effect of NaCl and H_2O was only recently explained by Ciszak et al. [17].

The objective of the present study is to better understand the influence of NaCl solid deposit on the oxidation behavior at high temperature (560 °C) of β21S Ti-based alloy. In this purpose, experiments in laboratory air and moist air were performed for 600 h. Corrosion products were analyzed by means of X-rays diffraction (XRD) and scanning electron microscopy (SEM) coupled to energy-dispersive X-ray spectroscopy (EDS) analysis, while oxygen dissolution area was identified through hardness measurements taken over the metallic material thickness.

Experimental Procedures

The β21S Ti-based alloys used for this study present the single β (CC) phase. It contains 15 wt% Mo, 3 wt% Nb, 3 wt% Al and 0.4 wt% Si. Rectangular samples (6 mm × 2 mm × 1 mm) were mechanically grinded on SiC papers up to 600 grit and were then cleaned in ethanol.

NaCl was deposited by spraying in several steps an aqueous saturated NaCl solution on the samples surfaces which were preheated at 60–80 °C. This method leads to a homogeneous and continuous deposit with a NaCl amount of 3–4 mg cm^{-2}.

Samples were exposed to laboratory air (0.5–1.5 vol% H_2O) in muffles furnaces. Air oxidation was performed at 560 °C for 600 h. Exposition to moist air [12 vol% $H_2O_{(g)}$] was done in an experimental tubular furnace at 560 °C for 600 h. Air enrichment in water vapor is performed by bubbling air in a round-bottom flask of distilled water heated at 100 °C, which leads to water vapor-saturated air. This mixture passes then through a condenser tube which is heated at 25 °C to set the

quantity of water vapor at 12 vol%, measured by a hygrometer. The steam then passes through the furnace tube with a flow of 8 ml min^{-1} (corresponding to a gas velocity of 0.75 cm s^{-1}).

All the samples were analyzed in two successive steps. Surfaces were first characterized, followed by cross sections analysis. Preparation of cross sections consists of several steps. At first, a thin layer of Au is sputtered on each sample's surfaces. Then, samples were coated with Cu by an electrolytic method. They are finally coated in carbon-doped phenolic resin and polished up to the mirror finishing.

The oxide surface and cross section morphologies were analyzed using a JEOL JSM-7600F scanning electron microscope. The chemical composition of the corrosion products was obtained by energy-dispersive X-ray spectroscopy (EDS). Phase composition of the oxide scales was determined by X-ray diffraction with an Inel CPS 120 diffractometer using Cu Kα ($\lambda = 0.154$ nm) radiation with fixed incidence angle of 1°. The Vickers micro-hardness of each sample was evaluated with a BUEHLER 1600–6100 setup using a charge of 10 g. Measurement points were marked on the whole thickness of the metallic material, each 10 μm near the surface (for the first 100 μm) and each 100 μm in the center of the sample.

Results

Samples Without Deposit Exposed to Laboratory Air and Water Vapor-Enriched Air

SEM cross section observations of β21S samples exposed to laboratory air (Fig. 1a) and moist air (Fig. 1b) for 600 h at 560 °C show homogeneous oxide layers that are adherent, continuous and composed of very small grains. Their thickness is low, of about 300 nm in the first case and 80 nm in the latter case. In both cases, EDS and

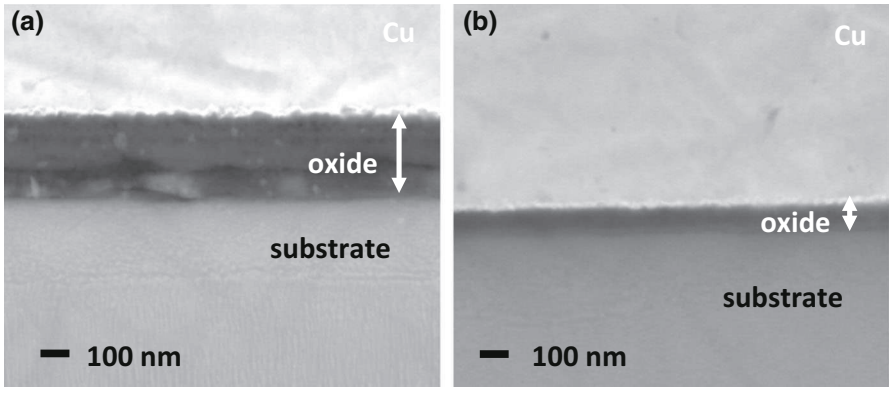

Fig. 1 SEM cross section observations after 600 h oxidation at 560 °C of β21S alloy in: **a** laboratory air, **b** moist air

surface XRD analyses indicate the presence of rutile TiO_2, as majority phase, and of a small quantity of anatase TiO_2.

Figure 2 presents the micro-harness and oxygen EDS profiles of β21S samples exposed to laboratory air (Fig. 2a) and moist air (Fig. 2b). A very high micro-hardness value, of 1085 $HV_{0.01}$, is obtained at the metal/oxide interface for the sample exposed to laboratory air, and a value of 955 $HV_{0.01}$ is measured at the equivalent location on the moist air sample. The hardness value decreases rapidly in both cases to reach the average value of the raw β21S alloy ($\sim$325 $HV_{0.01}$) at around 25 µm from the interface. At the same time, oxygen content decreases to reach a plateau at around 10 µm from the interface. It should be noted here that, because of the oxygen surface pollution, the oxygen content measured by EDS is certainly over-evaluated of several at%. Therefore, the oxygen content values shown in Fig. 2 should not be taken as quantitative; nevertheless, the existence of oxygen concentration profiles is evident as well after laboratory air and moist air exposures. By taking into account the micro-hardness evolution and the oxygen content variation, Fig. 2 allows evaluating the oxygen dissolution area thickness to be around 10 µm for both samples.

Samples with NaCl Solid Deposit Exposed to Laboratory Air and Water Vapor-Enriched Air

Surface SEM observations of β21S sample coated with NaCl and exposed to laboratory air for 600 h at 560 °C show a heterogeneous oxide layer presenting a large number of blisters (Fig. 3). EDS and XRD analyses indicate the presence of rutile TiO_2, as majority phase, and of $Na_4Ti_5O_{12}$, besides small amounts of TiO and Ti_2O.

The cross section observation (Fig. 4) of the sample shows that the oxide layer has a very important thickness that varies between 30 and 70 µm. Moreover, it is non-adherent to the metallic substrate, very brittle and affected by an important

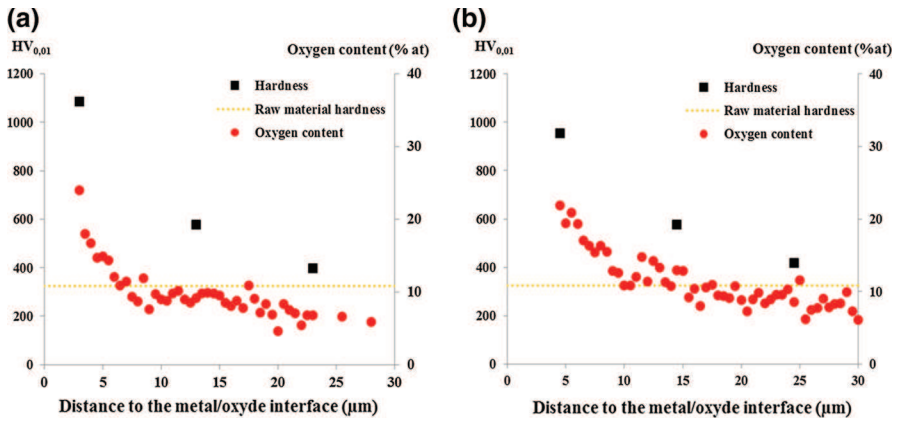

Fig. 2 Micro-hardness and relative oxygen content profiles versus distance from the metal/oxide interface for β21S oxidized at 560 °C for 600 h in: **a** laboratory air and **b** moist air

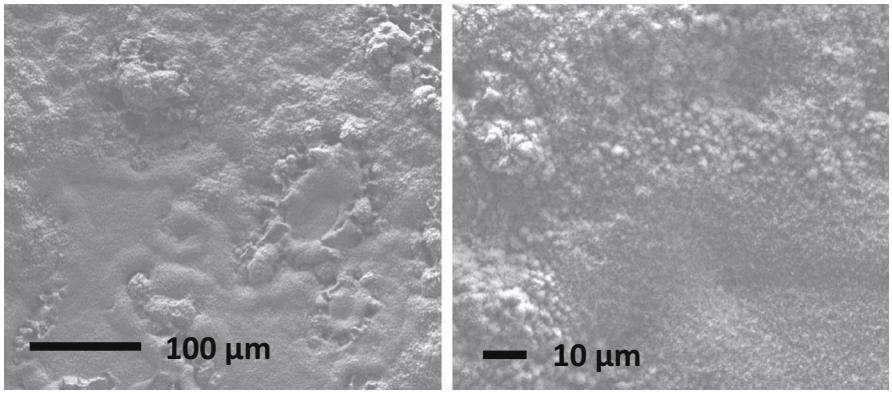

Fig. 3 SEM observations after 600 h laboratory air oxidation at 560 °C of β21S alloy with NaCl deposit

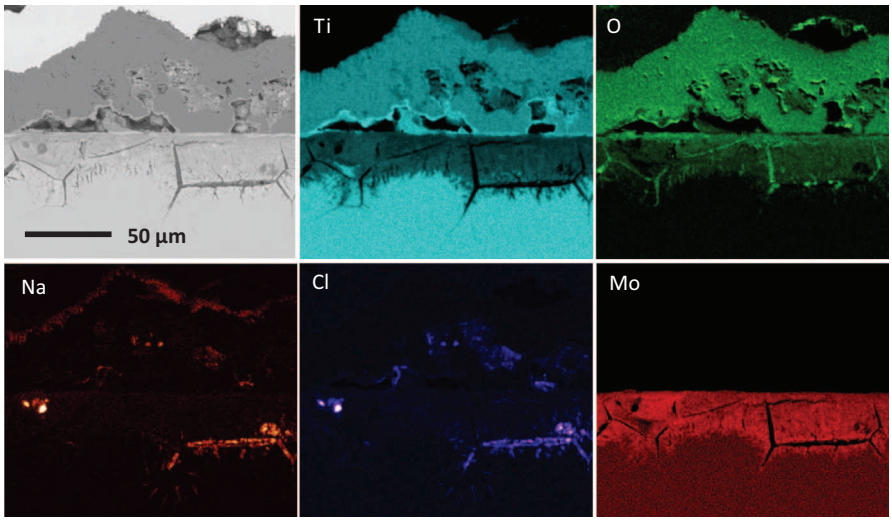

Fig. 4 Cross section SEM observations after 600 h laboratory air oxidation at 560 °C of β21S alloy with NaCl deposit

number of cracks and porosities. In parallel, an important cracking can be observed in the upper part of the substrate, within a layer of about 25 µm average depth.

EDS elementary mapping, also shown in Fig. 4, allows to identify the presence of Ti and O inside the entire corrosion scale. Na is present at the external part of the scale, while Na and Cl are detected together in the same regions inside the oxide layer and at the external part of the substrate. In the latter case, the simultaneous presence of Na and Cl corresponds to pores and cracks locations and indicates residues of the initial NaCl deposit, not removed during the washing step and partially redistributed during the polishing process. The external part of the oxide layer ($\sim$5 µm), where Na, Ti and O coexist, corresponds, in agreement with XRD results, to the location of the $Na_4Ti_5O_{12}$ oxide. The internal part of the oxide layer is

composed of Ti and O, and based on EDS quantification, it is possible to locate TiO_2 at its outer part, while the inner part should correspond to TiO and Ti_2O.

EDS elementary mapping in the outer part of the initial metallic substrate shows a very important Ti depletion inside the layer affected by cracking (60 at% instead of 84 at% in the Ti alloy). In consequence, more important atomic fractions of Mo (24 at% instead of 8 at%) and Al (16 at% instead of 5.7 at%) are observed in this region with respect to the nominal composition of the β21S alloy. Moreover, a very important presence of O was identified in this layer that varies between 60 at% in the outer part and 35 at% in the inner part. This very important amount of oxygen, that overcomes the dissolution limit of 33 at%, suggests the formation of oxide phases and not of an O-enriched metallic Ti layer. This conclusion was confirmed by micro-hardness measurements taken on cross section showing values close to the raw material hardness all over the thickness of the sample.

Very similar observations can be done concerning the β21S sample coated with NaCl and exposed to moist air for 600 h at 560 °C. The heterogeneous oxide layer presents a large number of blisters at its surface (Fig. 5). Cross section SEM images show that it is very brittle, is affected by cracks and pores and has a very poor adherence to the metallic substrate. Its thickness is very large, between 40 and 70 μm (Fig. 6). XRD analyses and EDS elementary mapping indicate that the corrosion scale is composed of a thin $Na_4Ti_5O_{12}$ layer at the external part, a thicker rutile TiO_2 layer in the middle part and a thin layer of $TiO_{0.7}$ at its inner part.

The cracking of the upper part of the initial substrate is again observed, in a region up to 35 μm average depth. EDS elementary mapping of this layer shows once more a very important Ti content diminution (53 at%), replaced by higher contents of Mo (29 at%) and Al (16 at%). Moreover, an important Mo enrichment of the grain boundaries can equally be observed. An important content of O is detected all over this area, between 60 and 40 at%, suggesting the formation of an oxide instead of an O-enriched layer in the metallic alloy. This observation is consistent

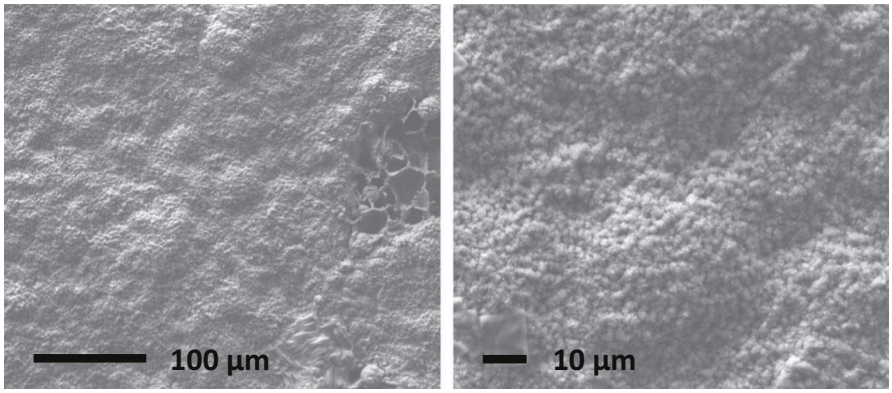

Fig. 5 SEM observations after 600 h moist air oxidation at 560 °C of β21S alloy with NaCl deposit

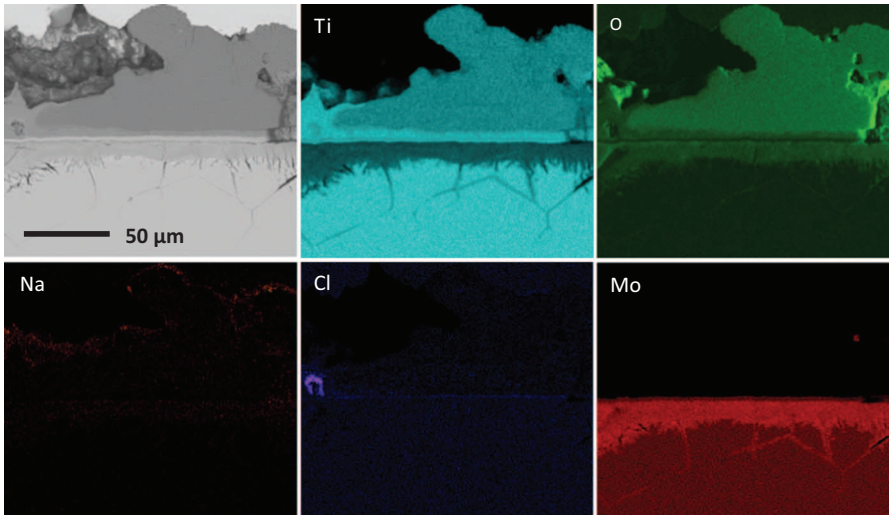

Fig. 6 Cross section SEM observations after 600 h moist air oxidation at 560 °C of β21S alloy with NaCl deposit

with the fact that constant micro-hardness values, close to raw material hardness, were measured in the metallic alloy, on the entire sample thickness.

Discussion

Table 1 summarizes the results obtained after exposure of β21S alloy without and with NaCl solid deposit for 600 h at 560 °C in laboratory air and moist air: the mass gain, the oxide layer thickness and the oxygen dissolution area thickness.

β21S alloy exposed to laboratory air presents a low mass gain and low oxide thickness, in agreement with the presence of alloying elements, Mo, Nb, Al and Si, having a positive impact on the oxidation behavior of Ti alloys [1, 3]. When exposed to moist air, its behavior is improved by decreasing the mass gain by a factor of 3 and the oxide thickness by a factor of 4 when compared to the similar exposure in laboratory air. This kind of evolution, in contradiction with Motte et al. and Wouters et al. works performed at higher temperatures [4, 5], was already observed by Champin et al. [3] at 600 °C on pure titanium and different titanium alloys.

The O-enriched layer has a similar thickness, independently of the water content in the gas. This observation suggests that the oxygen dissolution kinetics in the metal is independent of the external oxide layer thickness and is not affected by the potential presence in the metal of hydrogen coming from H_2O dissociation [18]. The fact that the O-enriched layer thickness does not depend on the thickness of the external TiO_2 scale is expected when considering that oxygen which dissolves into the metal comes from the dissociation of Ti oxide at the metal/oxide interface. When this dissolution is fast enough, the dissociation explains why neither TiO nor

Table 1 Mass gain, oxygen thickness and oxygen diffusion area thickness obtained after exposition in laboratory air and moist air at 560 °C during 600 h of β21S uncoated samples and of β21S samples with NaCl solid deposit

	Mass increase		Oxide thickness		Oxygen diffusion area	
	Laboratory air (mg cm^{-2})	Moist air (mg cm^{-2})	Laboratory air	Moist air	Laboratory air	Moist air
Without NaCl	0.43	0.18	300 nm	80 nm	10 μm	10 μm
With NaCl	3.42	5.98	30 − 70 μm + 25 μm*	40 − 70 μm + 35 μm*	–	–

* Internal oxidation of the β21S metallic substrate

Ti_2O is observed in the oxide scale, whereas they are expected at equilibrium (see Ti–O phase diagram). These phases are dissolved faster than they grow.

The presence of NaCl solid deposit at the surface of β21S alloy leads to a very harmful effect. The mass gain increases by a factor of 8 after oxidation in laboratory air and by a factor of 28 after exposure to moist air. In parallel, the oxide thickness is 250 times higher after laboratory air treatment and 1000 times higher after moist air exposure. These very important thickness variations can be related to the large porosity observed inside the corrosion scales obtained after oxidation in the presence of NaCl. Moreover, the blisters, cracks and the poor adherence of the oxide layer to the metallic substrate are complementary proofs of the detrimental behavior of β21S alloy in these conditions. The harmful effect is increased in the simultaneous presence of water vapor in the atmosphere and of NaCl deposit.

The results obtained in this study are in complete agreement with a previous study evaluating the behavior of Ti–6Al–4V alloy in identical experimental conditions [17]. The similar composition of the corrosion scales, with a thin $Na_4Ti_5O_{12}$ layer at the external part and TiO_2 at the inner part, suggests a similar corrosion mechanism for β21S as for Ti–6Al–4V in the presence of NaCl.

Thermodynamic calculations performed with Factsage 6.4™ software showed that, considering constant equilibrium between solid NaCl and gaseous NaCl, the NaCl vapor pressure at 560 °C is around 3×10^{-7} mbar; therefore, gaseous NaCl presence cannot be neglected. In parallel, Kwon et al. [20] showed that in the presence of NaCl solid deposits, reactions involve only gaseous NaCl. In consequence, a first reaction can be written in agreement with the present oxide phases:

$$4\ NaCl_{(g)} + O_{2\,(g)} + 5\ TiO_{2\,(s)} \leftrightarrow Na_4Ti_5O_{12\,(s)} + 2\ Cl_{2\,(g)} \quad (1)$$

This reaction is first supported by thermodynamical calculations showing that Cl_2 is the most important of the gas species formed during the reaction. Secondly, this reaction is in agreement with the calculated species predominance diagram that shows that in the high $P(O_2)$ and low $P(Cl_2)$ region, the decomposition of NaCl leads to the formation of a Na–Ti mixed oxide in the presence of TiO_2.

The chlorine released during reaction (1) can be partially diluted in the gaseous atmosphere, but some can migrate toward the metal/oxide interface and react with metallic Ti in order to form a Ti chloride:

$$Ti_{(s)} + 2\ Cl_{2\,(g)} \leftrightarrow TiCl_{4\,(g)} \quad (2)$$

This reaction is in agreement with the important depletion of Ti at the outer part of the metallic substrate, as shown in Fig. 4, and with the very high porosity observed near the metal/oxide interface.

The volatile $TiCl_4$ can be partially released, but can equally react with the oxygen that can easily arrive through the important cracks that formed inside the oxide layer. This reaction leads to the formation of rutile and production of gaseous chlorine:

$$TiCl_{4\,(g)} + O_{2\,(g)} \leftrightarrow TiO_{2\,(s)} + 2\,Cl_{2\,(g)} \quad (3)$$

The chlorine that forms during reaction (3) can then feed reaction (2): An active corrosion mechanism [19] is established, and these two reactions can take place indefinitely, as long as Ti can be provided, i.e., until the complete consumption of the alloy.

Similar reactions can be written when moisture is present in the exposure environment. The formation of $Na_4Ti_5O_{12}$ takes place with HCl release, that can subsequently react with metallic Ti to form $TiCl_4$ and H_2:

$$4\,NaCl_{(g)} + 2\,H_2O_{(g)} + 5\,TiO_{2\,(s)} \leftrightarrow Na_4Ti_5O_{12\,(s)} + 4\,HCl_{(g)} \quad (4)$$

$$Ti_{(s)} + 4\,HCl_{(g)} \leftrightarrow TiCl_{4(g)} + 2\,H_{2(g)} \quad (5)$$

The $TiCl_4$ resulting from reaction (5) can feed reaction (3) that will then lead again to the establishment of the active corrosion process based on reactions (2) and (3).

The synergistic effect of NaCl and H_2O can be explained by taking into account the hydrochloric acid released during reaction (4). Indeed, thermodynamical calculation showed that the mole fraction of HCl formed in moist air conditions is 1000 times higher than the mole fraction of Cl_2 formed during reaction (1) taking place in air. It results that the tank keeping up the active corrosion process is 1000 more important in moist air then the one available in laboratory air.

The role of hydrogen released by reaction (4) can equally be discussed, as it certainly contributes to the porosity and cracks formation inside the oxide layer. Furthermore, H_2O molecules can dissociate in H atoms and OH^- species. Their dissolution inside the oxide lattice will lead to a change of the defect chemistry and, in consequence, of the transport and growth processes [18].

The effect of NaCl solid deposit at β21S surface can equally be discussed in terms of oxygen dissolution area in the metal. In laboratory air as well as in moist air, the formation of O-enriched layer in the metal ("α-case") is replaced by the much faster inward transport of oxygen leading to the formation of a thick oxide phase scale. This considerable oxygen flow, facilitated by the numerous cracks present inside the corrosion layer, can be directly related to the very severe Ti depletion of the metallic substrate through the formation of volatile chlorides during the active corrosion process. The absence of oxygen dissolution in presence of NaCl suggests that the oxide layer growth is much faster than the kinetics of oxygen dissolution in the metal. Therefore, the TiO and Ti_2O oxide phases can be observed in the inner part of the oxide scale at equilibrium with the metal, because they grow faster than they are dissolved.

A synergistic effect of NaCl and H_2O can equally be pointed out through a larger thickness of affected metallic substrate: an average of 35 μm in the presence of moist air compared to 25 μm in laboratory air. The consequences of the active corrosion in the presence of NaCl solid deposit on the mechanical properties of β21S alloy should be evaluated in the future.

Conclusions

Laboratory air and moist air oxidation behaviors of β21S Ti-based alloys were evaluated after 600 h at 560 °C. In both atmospheres, the corrosion layers are very thin. The presence of moisture has a positive effect on β21S oxidation. Nevertheless, the kinetics of growth of the O-enriched layer in the metallic substrate is similar in both cases.

The presence of a solid NaCl deposit at the surface of β21S alloy has a very harmful effect, leading to a very important increase of the mass gain and of the corrosion product layer thickness. This effect was explained through the establishment of an active corrosion mechanism. The synergistic effect of NaCl and H_2O was observed and related to the important production of HCl in moist air conditions. The presence of NaCl avoids the formation of the brittle O-enriched metallic layer ("α-case"); a very cracked oxide layer forms instead at the external part of the metallic substrate. Its influence on the mechanic properties of the β21S alloy should be evaluated. It is not obvious to know in advance if the thicker corrosion product observed in the presence of NaCl is more damaging than the embrittlement due to oxygen diffusion in the metallic matrix without NaCl.

Acknowledgements The authors would like to thank Frédéric HERBST, Nicolas GEOFFROY and Nathalie ROUDERGUES for technical support and Michel VILASI and Stéphane MATHIEU (Institut Jean Lamour, Nancy) for fruitful discussions.

References

1. G. Lütjering, J. C. Williams, *Titanium*, ed. (Springer, Berlin, 2007), pp. 50–51.
2. I. Gurrappa, *Oxidation of Metals* **59**, 2003 (321–332).
3. B. Champin, L. Graff, M. Armand, G. Béranger and C. Coddet, *Journal of Common Metals* **69**, 1980 (163–183).
4. F. Motte, C. Coddet, P. Sarrazin, M. Azzopardi and J. Besson, *Oxidation of Metals* **10**, 1976 (113–126).
5. Y. Wouters, A. Galerie and J. P. Petit, *Solid State Ionics* **104**, 1997 (89–96).
6. H. L. Du, P. K. Datta, D. B. Lewis and J. S. Burnell-Gray, *Oxidation of Metals* **45-5**, (6), 1996 (507–527).
7. D. Poquillon, C. Armand and J. Huez, *Oxidation of Metals* **79**, 2013 (249–259).
8. S. R. J. Saunders, M. Monteiro and F. Rizzo, *Progress in Material Science* **53**, 2008 (775–837).
9. J. Stringer, *Acta Metallurgica* **8**, 1960 (758–766).
10. P. Perez, *Corrosion Science* **49**, 2007 (1172–1185).
11. G. Sanderson and J. C. Scully, *Corrosion Science* **8**, 1968 (771–777).
12. P. Dumas and C. S. John, *Oxidation of Metals* **10**, 1976 (127–134).
13. Z. Yao and M. Marek, *Materials Science and Engineering A* **192**, 1995 (994–1000).
14. Y. Xiong, S. Zhu and F. Wang, *Corrosion Science* **50**, 2008 (15–22).
15. Y. Shu, F. Wang and W. Wu, *Oxidation of Metals* **52**, 1999 (463–473).
16. D. Zheng, S. Zhu and F. Wang, *Surface and Coating Technology* **201**, 2007 (5859–5864).
17. C. Ciszak, I. Popa, J. M. Brossard, D. Monceau and S. Chevalier, *Corrosion Science* **110**, 2016 (91–104).
18. A. Zeller, F. Dettenwanger and M. Schütze, *Intermetallics* **10**, 2002 (59–72).
19. H. J. Grabke, E. Reese and M. Spiegel, *Corrosion Science* **37**, 1995 (1023–1043).
20. J. W. Kwon, Y. Y. Lee and Y. D. Lee, *Materials at High Temperatures* **17**, 2000 (319–326).